Electronic Supplementary Material (ESI) for Lab on a Chip.

Supplemental Information

1 Supplemental Methods

1.1 Testing the Effects of Electroporation Media Exposure Time on Bulk Electrotransfection Efficiency and Viability

Primary human T cells from 3 separate, independent donors were used to test the effects of electroporation media exposure time on transfection efficiency and post-transfection viability for BTXpress media and mRNA cargo. Isolated T cells were thawed and cultured as described in section 3.3. T cells were washed once with PBS and then resuspended in BTXpress media at a concentration of 5 x 10^6 /mL. 50 µg/mL of Trilink mCherry mRNA was added to the cell suspension, and then 200 µL of the final mixture was transferred into electroporation cuvettes with a 4-mm gap (BTX Electroporation Cuvettes Plus, Yellow). The zero-minute time point cuvette was electroporated immediately in a BTX Gemini X2 using the human T cell setting (500V, 0.7ms, 1 Pulse, Square wave). For the 15 and 60-minute time points, cuvettes were loaded and then left undisturbed at room temperature for the indicated time, and then electroporated using the same setting. Electroporated samples were plated into TexMACS Medium (Miltenyi Biotec) containing 1% penicillin-streptomycin (Thermofisher), and 100 U/mL Human IL-2 (Miltenyi Biotec), at an approximate density of 1 x 10^6 /mL. Flow cytometry was performed after 24 hours to measure transfection efficiency and viability as described in section 3.13.

1.2 Measurement of Diffusive Mixing of Laminar Streams using Fluorescence

Sodium fluorescein was dissolved in PBS solution at a concentration of 10 ng/mL. The fluorescent PBS solution was introduced into the sheath inlet at a combined flow rate of 60 µl/min to generate the sheath streams in the device, and BTX was introduced into the center inlet at a flow rate of 40 µL/min. Sheath and center outputs were collected separately, and 100 µL of each collection sample were analyzed using a Synergy H1 microplate reader from BioTek. A green filter with excitation 485/20 nm and emission 528/20 nm was used. Samples were collected first with the acoustic excitation turned off, and then with the excitation turned on in order to determine if the application of the acoustic field was generating any undesired mixing. Concentrations were computed from fluorescence measurements by comparison to a standard curve.

2 Supplemental Results

2.1 Effect of Cell Holding Time in Electroporation Media on Transfection Efficiency and Post-Transfection Viability

Primary human T cells were held in BTX electroporation buffer with mCherry mRNA for 0, 15 and 60 minutes and then electroporated using a BTX Gemini commercial electroporator. Flow cytometry analysis after 24 hours showed a statistically significant difference ($p = 0.0069$, paired t-test) in mCherry transfection efficiency after T cells were left undisturbed in a cuvette for 15 minutes (77.8% at t = 0 vs. 59.1% at t = 15 min). There was also a significant difference ($p = 0.0014$, paired t-test) in transfection between the 15-min and 60-min time points, where the transfection efficiency dropped from , 59.1% to 6.8%. There were no statistical differences between the different hold time conditions in post-transfection viability.

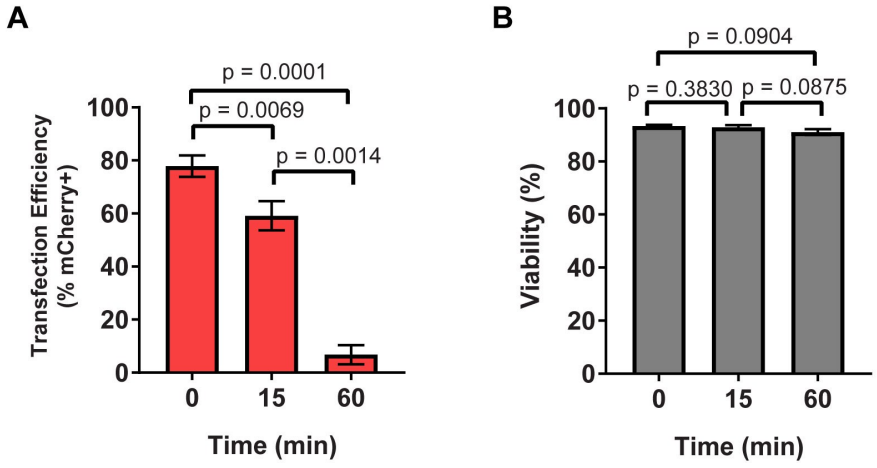

Figure S1. *Primary human T cells were electroporated after being held in BTX electroporation media for 0, 15, or 60 minutes. Data is the average of replicates from 3 independent, healthy donors, and error bars represent the standard error of the mean. (A) Transfection efficiency, as measured by flow cytometry 24 hours after electroporation, is reduced when T cells are held in BTXpress media with mRNA for 15 min, and is reduced further if the hold time is increased to 60 min. (B) Post-transfection viability, as measured by flow cytometry 24 hours after electroporation, decreases with increasing hold time, but the decrease is not statistically significant.*

2.2 Coupling of Acoustic Mode to Elastic Deformation of Channel Walls

In our device, the acoustic contrast between the polystyrene walls and the fluid-filled channel is sufficiently small that the acoustic mode in the channel is strongly coupled to the elastic deformation of the channel walls in response to the acoustic stimulation. The joint waveform of the entire device determines the resonant frequency at which optimal focusing of cells to the center of the channel is found, rather than this being determined solely by the waveform within the channel as would be the case for a rigid walled channel with high acoustic impedance mismatch. This effect has been explored at length by Moiseyenko and Bruus[1] and is demonstrated in our simulations of the acoustic behavior of the channel in Figure S2. Both the inner channel dimensions, and outer dimensions of the polystyrene block are set to match the experimental conditions, and both are important for determining the overall resonant behavior of the device.

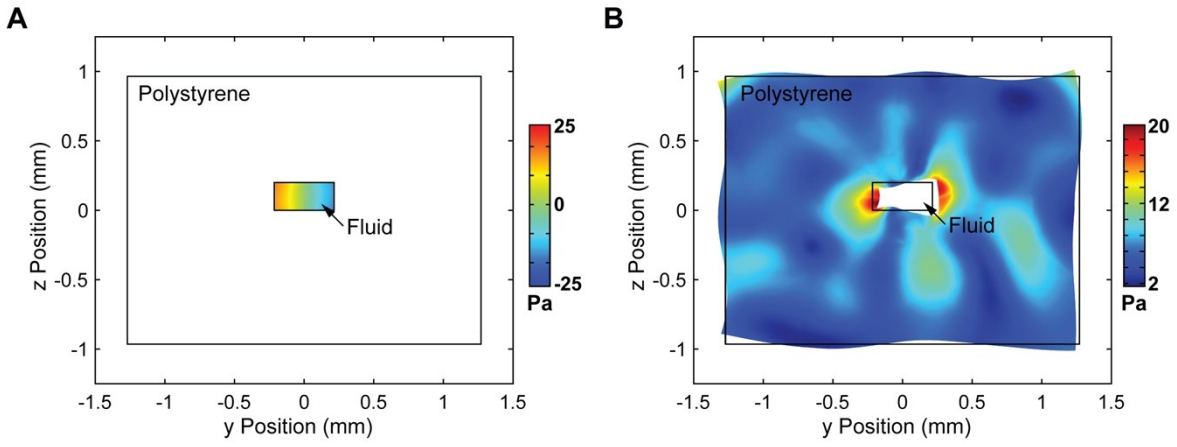

Figure S2*. (A) Acoustic pressure in a YZ cross section of the channel at x = 10.5 mm with a focusing frequency of 933 kHz. (B) For the same cross section, von Mises stress and displacement with a scale factor of* $5x10^7$ *are plotted demonstrating the coupling between the acoustic pressure in the channel and the distortion of the polystyrene walls.*

2.3 Assessment of Mixing Using Fluorescein Solution

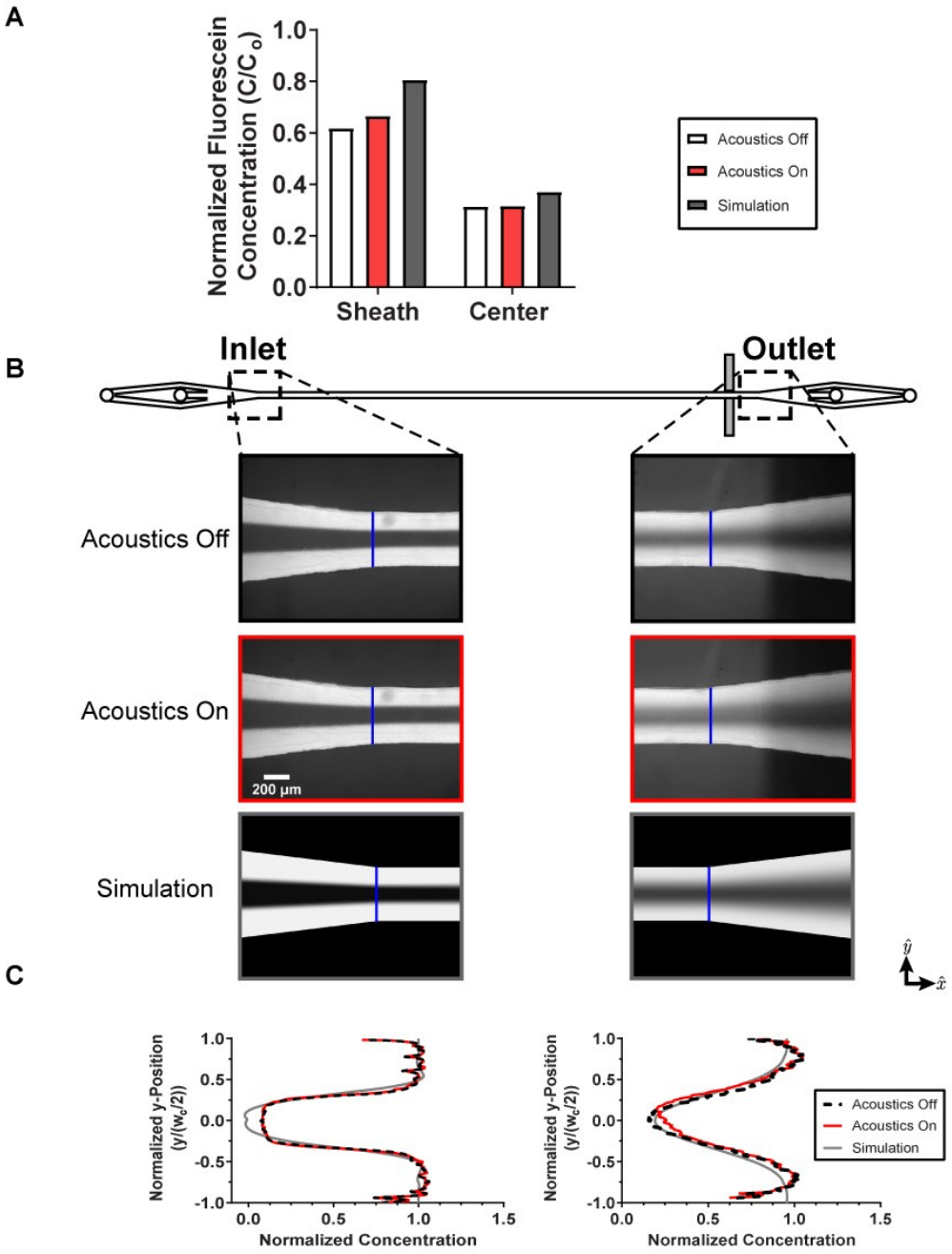

Figure S3. *Acoustic stimulation does not disrupt the laminar sheath flow or cause mixing of the streams beyond diffusion. Sodium fluorescein dissolved in PBS solution was flowed into the sheath streams at 60 µL/min, and BTX solution was flowed into the center stream at 40 µL/min. (A) The fluorescence of fluid collected independently from the sheath and center outlets was measured using a fluorescence plate reader. (B) Top-down views of the inlet and outlet regions of the device at positions indicated by the dotted box on the device schematic. Images are shown with the acoustics off (black box), the acoustics on (red box), and for the simulated concentration distribution (grey box). For these images, sodium fluorescein in PBS solution was introduced into the sheath streams and BTX solution was introduced into the center stream. The blue vertical lines in the images indicate the positions where we measured fluorescence intensity profiles across the channel width (at x = -17mm and x = +17mm). (C) Normalized fluorescence intensity as a function of position across the width of the channel with acoustics turned off and on. Position along the y-axis was normalized by the half-width of the channel. Simulation data is also included for comparison.*

For a second assessment of mixing without cells in the system, we flowed a solution comprised of sodium fluorescein dissolved in PBS solution into the sheath streams, and non-fluorescent BTX solution into the center stream. We measured the fluorescence of fractions collected at the sheath and center stream using a fluorescence plate reader (Figure S3A); these data followed trends similar to those seen in the conductivity measurements where differences between fractions collected with and without acoustic stimulation were minimal (Figure 6). We also analyzed fluorescence microscopy images to measure the spatial distribution of the dye in the microchannel (Figure S3B). From analysis of the fluorescence images, we determined that acoustic stimulation did not affect the spatial distribution of the fluorescence. We specifically examined positions near the inlet of the device (x = -17 mm) and near the outlet (x = 17 mm), and found that the evolution of the fluorescence intensity profile across the width of the channel was well-described by a pure diffusion model (Figure S3C). This is confirmed by good agreement with data from our transport simulations, which included diffusion but did not include acoustic stimulation.

References

1 R. P. Moiseyenko and H. Bruus, *Phys. Rev. Appl.*, 2019, **11**, 14014.